Identification of Residues Lining the Anthrax Protective Antigen Channel[†]

Ericka L. Benson,[‡] Paul D. Huynh,[§] Alan Finkelstein,[§] and R. John Collier*,[‡]

Department of Microbiology and Molecular Genetics, Harvard Medical School, 200 Longwood Avenue, Boston, Massachusetts 02115, and Departments of Physiology & Biophysics and Neuroscience, Albert Einstein College of Medicine, 1300 Morris Park Avenue, Bronx, New York 10461

Received October 27, 1997; Revised Manuscript Received January 13, 1998

ABSTRACT: In its activated 63 kDa form, the protective antigen (PA) component of anthrax toxin forms a heptameric prepore, which converts to a pore (channel) in endosomal membranes at low pH and mediates translocation of the toxin's enzymic moieties to the cytosol. It has been proposed that the prepore-to-pore conversion involves a conformational rearrangement of a disordered amphipathic loop (D2L2; residues 302−325), in which loops from the 7 protomers combine to form a transmembrane 14-stranded β barrel. To test this model, we generated Cys substitutions in 24 consecutive residues of the D2L2 loop, formed channels in artificial bilayers with each mutant, and examined changes in channel conductance after adding the thiol-reactive, bilayer-impermeant reagent methanethiosulfonate ethyltrimethylammonium (MTS-ET) to the trans compartment. The rationale for these experiments is that reaction of MTS-ET with a Cys residue adds a positively charged group and therefore would likely reduce channel conductance if the residue were in the ion-conducting pathway. We found alternating reduction and absence of reduction of conductance in consecutive residues over two stretches (residues 302−311 and 316−325). This pattern is consistent with alternating polar and apolar residues of the two stretches projecting into the pore lumen and into the bilayer, respectively. Residues connecting these two stretches (residues 312−315) were responsive to MTS-ET, consistent with their being in a turn region. Single channels formed by selected mutants (H304C and N306C) showed multiple conductance step changes in response to MTS-ET, consistent with an oligomeric pore. We also found that the binding site for the channel-blocking tetraalkylammonium ions is located cis relative to the inserted D2L2 loops. These findings constitute strong evidence in favor of the model of conversion of the prepore to a 14-stranded β barrel pore and solidify the foundation for studies to understand the mechanism of translocation by anthrax toxin.

Intracellularly acting bacterial toxins must cross a membrane barrier of host cells to reach their cytosolic targets. Most intracellularly acting toxins may be classified as A−B toxins, where the B moiety binds to the surface of the host cell and translocates the enzymatic A moiety into the cytosol (*1*). In many of these toxins, membrane translocation of the A moiety involves insertion of the B moiety into the host membrane, resulting in the formation of an ion-conducting pore. X-ray crystal structures have been solved for the water-soluble forms of two pore-forming A−B toxins and also of other toxins that function simply by forming pores at the cell surface (*2*−*6*). The crystal structure of one pore-forming toxin has been solved in its membrane-inserted form (*7*). Membrane insertion by these water-soluble proteins involves conformational changes to expose or generate new surfaces which can penetrate hydrophobic membrane barriers. In the case of pore-forming A−B toxins, it is unclear whether the pore formed by the B moiety serves as a conduit for translocation or is a byproduct of membrane penetration.

In anthrax toxin, the A and B moieties are separate proteins which self-assemble at the mammalian cell surface. The B moiety, protective antigen (PA),[1] mediates the translocation of two alternative A moieties, edema factor (EF) and lethal factor (LF), into the cytosol. Under the current model for anthrax intoxication, PA first binds to a ubiquitous cell surface receptor (*8*) and is then cleaved by furin or a furin-like protease (*9*). Proteolytic removal of the N-terminal 20 kDa fragment enables the remaining receptor-bound 63 kDa fragment (PA_{63}) to form a heptameric prepore (*10*) and to bind EF or LF (*11*). The entire complex is then trafficked to the endosome, where the low-pH environment induces the PA_{63} prepore to insert into the membrane and translocate EF and LF to the cytosol (*12*, *13*). In the cytosol, both EF and LF catalyze reactions that have toxic effects (*14*, *15*).

Insertion of the PA_{63} heptamer into the endosomal membrane is believed to mediate translocation of EF and LF, and elucidation of the insertion mechanism is crucial for understanding the translocation process. Under low-pH conditions, PA_{63} forms cation-selective channels in artificial membranes (*16*, *17*) and in cell membranes (*18*). Purified PA_{63} was originally shown by electron microscopy to form

[†] This work was supported by NIH grants T32-GM07288 (P.D.H.), GM29210 (A.F.), and AI22021 (R.J.C.).

* To whom correspondence should be addressed.
[‡] Harvard Medical School.
[§] Albert Einstein College of Medicine.

[1] Abbreviations: Bu_4N^+, tetrabutylammonium; DTT, dithiothreitol; EDTA, ethylenediaminetetraacetic acid, disodium salt; EF, edema factor; D2L2, loop 2 of domain 2 in PA; LF, lethal factor; MTS-ES, methanethiosulfonate ethyl sulfate; MTS-ET, methanethiosulfonate ethyltrimethylammonium; PA, protective antigen; PA_{63}, C-terminal 63 kDa tryptic fragment of PA.

S0006-2960(97)02657-3 CCC: $15.00
Published on Web 02/26/1998

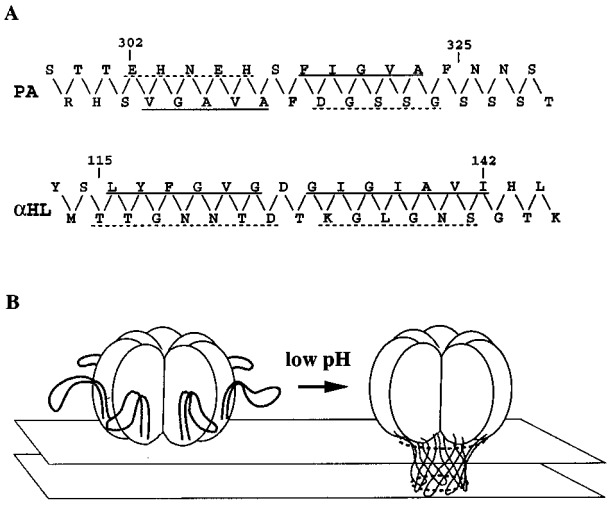

FIGURE 1: (A) Amphipathic sequences of the D2L2 loop of PA [after Petosa et al. (1997)] and the Gly-rich loop of α-hemolysin (αHL). Residues that form the hydrophobic face of the β barrel in α-hemolysin, or have been proposed to form the hydrophobic face of the PA_{63} pore, are underscored with a solid line. Residues that form the hydrophilic face in α-hemolysin, or have been proposed to form the hydrophilic face of the PA_{63} pore, are underscored with a dotted line. (B) Proposed model for pore formation by PA_{63} [after Petosa et al. (1997)]. Following a low-pH trigger, the D2L2 loops move to the base of the heptamer and combine to form a 14-stranded transmembrane β barrel.

ring-shaped heptamers (*10*), and recently the X-ray crystal structure of a heptameric, water-soluble form of PA_{63} was determined (*6*). Since this structure shows no regions of hydrophobicity that might mediate membrane insertion, we believe it represents an intermediate, or prepore, in the insertion process.

Potential clues to the mechanism of insertion by the PA_{63} prepore come from studies of the bacterial pore-forming toxin α-hemolysin from *Staphylococcus aureus*. This toxin, which shows no sequence similarities to PA, forms a heptameric pore in membranes (*19*). The recently reported crystal structure of the pore indicates that the transmembrane motif consists of a porin-like 14-stranded β barrel formed from 7 β hairpins (*7*). One β hairpin is contributed by each of the protomers, and each hairpin is in turn derived from a Gly-rich amphipathic loop in the monomeric water-soluble protein. The loop contains alternating hydrophilic and hydrophobic residues. Once assembled into the membrane-penetrant β barrel, the hydrophilic residues face the aqueous lumen of the pore, and the hydrophobic residues form the exterior, membrane-contiguous surface of the barrel.

The crystal structures of native PA and the PA_{63} prepore reveal the presence of a disordered, amphipathic loop (D2L2), which has alternating hydrophilic and hydrophobic residues reminiscent of the Gly-rich loop of the α-hemolysin (Figure 1A). This loop, which connects strands 2β2 and 2β3 within domain 2, projects outward from the side of domain 2 of each monomer within the water-soluble heptamer (*6*). A significant conformational rearrangement would be needed for this loop to participate in barrel formation, but a plausible mechanism for such a rearrangement has been proposed (Figure 1B) (*6*).

To determine whether D2L2 forms a transmembrane β barrel channel similar to that of the α-hemolysin, we employed the substituted cysteine accessibility method (*20*) to the 24 residues of this loop. In this method, individual residues are replaced with cysteine and tested for accessibility to bilayer-impermeant methanethiosulfonate derivatives which specifically react with water-accessible sulfhydryls. PA is ideally suited to this method, in that the native protein is devoid of cysteines. For these studies, we employed the positively charged reagent methanethiosulfonate ethyltrimethylammonium (MTS-ET). Should the cysteine of interest line the ion-conducting pathway, derivatization with MTS-ET would introduce a positive charge within the cation-selective channel and likely result in reduction of channel conductance. This method has been used to identify channel-lining residues of many proteins, including the nicotinic acetylcholine receptor (*21*), the $GABA_A$ receptor (*22*), the CFTR channel (*23*), K^+ channels (*24*, *25*), and the diphtheria toxin channel (*26*). The results reported below provide strong evidence in favor of the proposed model of membrane penetration by PA_{63} to form a β barrel pore.

EXPERIMENTAL PROCEDURES

Materials. MTS-ET bromide and sodium MTS-ES were generous gifts from Dr. David Stauffer; Bu_4N bromide, puriss grade, was obtained from Fluka.

Construction and Purification of Cysteine Mutants. Wild-type PA, containing a conservatively introduced *Sal*I site at 792 bp, was cloned into the *Bam*HI−*Xho*I sites of the *Escherichia coli* expression vector pET22b$^+$ (Novagen), which directs for periplasmic expression. Site-directed mutants were created from this template via two-step recombinant PCR using appropriate primers, and a 195 base pair *Sal*I−*Eco*RI fragment was subcloned back into the wild-type vector. The ligation products were transformed into *E. coli* XL1-Blue (Stratagene). The plasmid DNA was amplified, purified, and sequenced to confirm the presence of the mutation. Confirmed mutant plasmids were then transformed into the *E. coli* expression host BL21(DE3). Cultures were grown in Luria broth containing ampicillin at 37 °C to an OD_{600} of 0.6−1.0, and protein expression was induced by addition of isopropyl β−D-thiogalactopyranoside (1 mM) for 3 h at 30 °C. Periplasmic proteins were extracted by first resuspending pelleted cells in 4 mL of 20% sucrose, 5 mM EDTA, 150 μg/mL lysozyme, 20 mM Tris-HCl, pH 8.0, per gram of cells. After incubation on ice for 40 min, 80 μL of 1 M $MgCl_2$ per gram of cells was added. The mixture was centrifuged, and the resulting supernatant containing the desired protein was dialyzed overnight in buffer A (20 mM Tris, pH 8.0, 2 mM DTT, 1 mM EDTA). The protein was then purified by anion exchange chromatography (Q-Sepharose followed by Mono Q) in buffer A. Occasionally, a further gel filtration step (Superdex 75) in buffer A containing 150 mM NaCl was required. Proteins were purified to 90% homogeneity, as judged by SDS−PAGE. Approximately 0.5 mg of purified protein was obtained from 1 L of cells. Proteins were stored in 2 mM DTT at −80 °C until use.

Trypsin Activation of Cysteine Mutants. Mutant proteins were diluted to 0.5 mg/mL in buffer A, and trypsin was added to a final concentration of 1 μg/mL. After incubation for 5 min at 37 °C, soybean trypsin inhibitor was added to a final concentration of 10 μg/mL. Nicked proteins were stored on ice or at −80 °C until use. Although the mutant proteins

were stored in 2 mM DTT, it was found that maximal channel-forming activity and cysteine reactivity toward MTS-ET was obtained if fresh DTT, to an additional 2−5 mM, was added to the nicked samples each day of use.

Macroscopic Channel Experiments. Macroscopic conductance experiments were carried out at room temperature on planar lipid bilayers formed by the brush technique of Mueller et al. (1963) across a 0.5 mm diameter hole in a Teflon partition separating two Lucite compartments containing 3 mL of identical salt solutions (100 mM KCl, 1 mM EDTA, 10 mM dimethylglutaric acid, pH 6.6). The membrane-forming solution was 3% diphytanoylphosphatidylcholine in decane. After the membrane formed, trypsin-nicked mutant PA was added to the cis compartment to a final concentration of 30 pM to 3 nM (the final concentration of DTT in that compartment was typically 0.1−1 μM). Each compartment was stirred continuously throughout the experiment by small magnetic stir bars. After the mutant PA-induced current had stabilized, typically after 3−5 min, MTS-ET was added either to the cis compartment to a final concentration of 4 μM or to the trans compartment to a final concentration of 4−160 μM; these concentrations of MTS-ET had no effect on the current induced by nicked wild-type PA. The effects of MTS-ET on mutant PA-induced conductance generally occurred over a period of tens of seconds. The percent decline of conductance produced by MTS-ET was calculated as $[1 - (I_{PA+MTS}/I_{PA})] \times 100$, where I_{PA} was the current immediately before MTS-ET addition and I_{PA+MTS} was the lowest current observed within 3 min following addition of MTS-ET. Values are reported as the mean ± standard error of 2−4 experiments. In experiments involving Bu_4N^+, this reagent was added to a final concentration of 15 μM cis or 500 μM trans. All experiments were done under voltage clamp conditions (with the cis compartment held at +20 mV with respect to the trans compartment), using a single pair of Ag/AgCl electrodes that made electrical contact with the solutions in the compartments through 3 M KCl agar bridges. The current responses were filtered at 10 Hz and displayed on a Narco physiograph chart recorder.

Single-Channel Experiments. Planar bilayers were formed at room temperature from a 1% solution of diphytanoylphosphatidylcholine in hexane using a modification of the folded film method (*27*) across a 90−100 μm hole in a polystyrene cup (*28*) as previously described (*29*). The solutions both inside (0.5 mL) and outside (1 mL) the cup were the same as in the macroscopic experiments and could be stirred by small magnetic stir bars. Experiments were performed under voltage clamp conditions at +50 mV cis. In a typical experiment, nicked mutant PA was added, after the membrane formed, to a final concentration of 150 pM−16 nM to the outside compartment (cis), and the resulting current responses were monitored on a chart recorder and recorded on digital tape as previously described (*29*). After a channel appeared, MTS-ET was added to the trans compartment to a concentration of ~1 μM. Solutions were stirred as necessary. For the DTT reversal experiments, DTT was subsequently added to the trans compartment to a final concentration of ~1 mM.

RESULTS

Macroscopic Conductance Measurements. A series of 24 mutations, each replacing an individual D2L2 residue with cysteine, was generated via recombinant PCR. DNA fragments encoding the desired mutation were subcloned into wild-type PA within the pET22b$^+$ vector, and the mutant proteins were expressed in *E. coli*, harvested from the periplasm, and purified via anion exchange and gel filtration chromatography to 90% homogeneity.

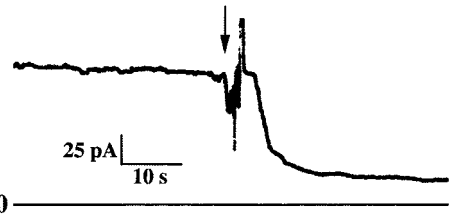

FIGURE 2: Effect of MTS-ET on N306C-induced macroscopic conductance. The current record (with the voltage held at +20 mV) begins 7 min after addition of trypsin-nicked PA N306C to a final concentration of 1.1 nM. At the arrow, MTS-ET was added trans to a concentration of 38 μM. After the initial artifactual increase in conductance due to the addition, the current is seen to decrease 6-fold within seconds.

PA is cleaved in vitro into its 20 and 63 kDa fragments by treatment with trypsin. When trypsin-activated PA is added to artificial lipid bilayers and the pH is reduced below pH 7 in the presence of 1 mM EDTA, cation-selective channels are formed, which are identical to those formed by purified PA_{63} (*16*). All of the D2L2 cysteine mutant proteins formed channels in planar lipid bilayers as readily as wild type, provided they had been activated with trypsin and fully reduced.

For macroscopic conductance experiments, in which the collective conductance of hundreds to thousands of channels is measured, subnanomolar to nanomolar concentrations of trypsin-activated mutant were added to painted diphytanoylphosphatidylcholine bilayer membranes held at a voltage of +20 mV at pH 6.6. Once the current had more or less plateaued, MTS-ET was added to the trans compartment (the compartment opposite that to which PA was added), and its effect on macroscopic current was observed. The positively charged methanethiosulfonate reagent MTS-ET was chosen because of the known cation selectivity of PA_{63} channels. For certain mutants, an immediate and large decline in current was observed, whereas for others no decline was detected, even after several minutes. Figure 2 shows a typical trace for a MTS-ET-responsive mutant. Addition of 38 μM MTS-ET trans to channels formed by the N306C mutant reduced the macroscopic current nearly 6-fold within seconds. Subsequent trans addition of 4 mM DTT caused a reversal of the effect (data not shown). The current induced by most other MTS-ET-responsive mutants was also maximally reduced within seconds following MTS-ET addition. With some mutants, the decrease was more gradual, but in all cases was essentially complete within 3 min. The reduced current persisted with most mutants for the duration of the experiment. [In some experiments, the decline in G317C- and S319C-induced current produced by MTS-ET added trans was followed by a linear rise in current to levels exceeding that which was observed before MTS-ET addition (data not shown). The reasons for this effect are unknown, but it is conceivable that reaction of MTS-ET at these sites catalyzes disulfide formation between monomers which could alter channel structure to a state of higher conductance.] Neither MTS-ET nor DTT, at the concentra-

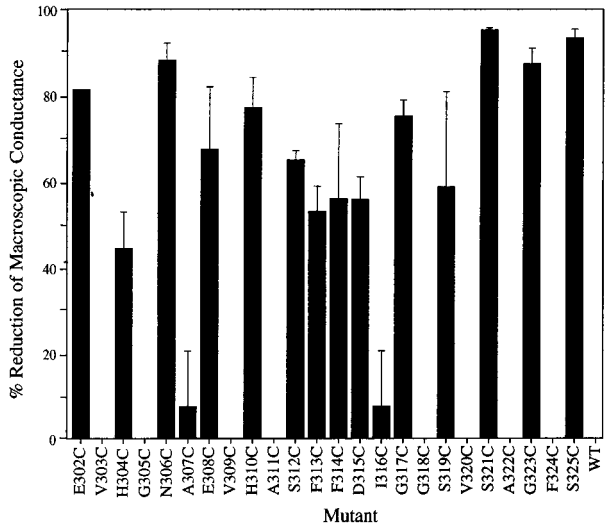

FIGURE 3: Reduction of conductance produced by trans MTS-ET as a function of the location of Cys mutants within the D2L2 loop. Percent reduction was calculated as $[1 - (I_{PA+MTS}/I_{PA})] \times 100$, where I_{PA} was the current immediately before MTS addition and I_{PA+MTS} was the lowest current observed within 3 min following addition of MTS-ET. Values are reported as the mean ± standard error of 2−4 experiments. For A307C and I316C, MTS-ET-induced reduction in current was only seen in some experiments. Note the alternating pattern of reduction in conductance, except for the consecutive MTS-ET-responsive residues 312−315. A similar pattern was seen when MTS-ET was added cis (data not shown).

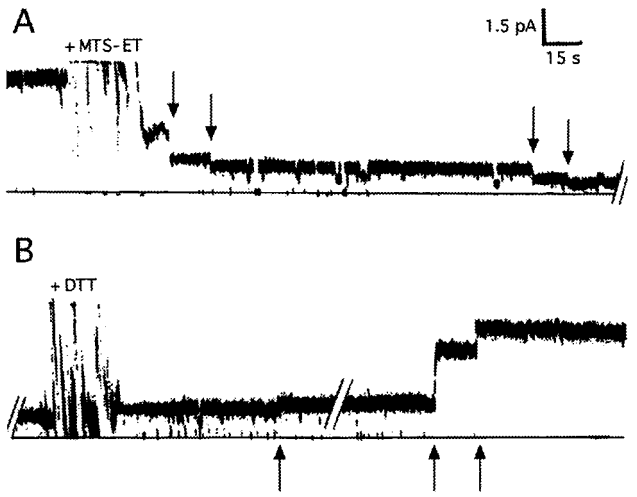

FIGURE 4: (A) Effect of MTS-ET on conductance of a single N306C channel. The trace begins after a single channel has opened with a conductance of 90 pS (at a holding potential of +50 mV). MTS-ET was then added to a concentration of 8 μM trans, and the current record was briefly obscured during stirring. One or more reactions occurred during stirring, since after the stirring was stopped the conductance of the channel was about half that before MTS-ET addition. The arrows indicate stepwise decreases in single-channel conductance consistent with the reaction of MTS-ET with cysteines within the channel. (B) DTT reverses the MTS-ET effect. The trace begins 5 min after the final MTS-ET reaction was observed in (A). DTT was added trans to a concentration of 1.2 mM, and the single-channel conductance immediately increased during stirring. The arrows indicate further stepwise increases in single-channel conductance, consistent with reduction of the mixed disulfides formed upon reaction of the cysteines with MTS-ET. At higher time resolution, the transition at the second arrow appears to be composed of 2−4 stepwise increases in conductance. (The last break in the record is 90 s.)

tions used in these experiments, showed any effect on wild-type channels.

Figure 3 shows the maximal reduction of macroscopic current attained by each mutant within the first 3 min following trans addition of MTS-ET. Within each of two stretches of D2L2 (E302C−A311C and I316C−S325C), alternating positions displayed a reduction of current following the addition of MTS-ET. All hydrophilic positions within these stretches were responsive to MTS-ET, whereas all hydrophobic positions displayed little to no MTS-ET effect. (The only exceptions were positions A307C and I316C, where a slow effect was seen in some experiments.) These stretches were bridged by a region of consecutive MTS-ET-responsive residues, from S312C−D315C. The pattern of current reduction was identical when MTS-ET (~4 μM) was added to the cis side (data not shown). When methanethiosulfonate ethyl sulfate (MTS-ES, ~100 μM), which adds a negatively charged sulfate group to a reactive cysteine, was added in place of MTS-ET, the responses of the mutant channels were more variable: reduction of current was seen at some positions, and increase of current was seen at other positions, including all sites where a negatively charged native residue (E302, E308, and D315) had been replaced (data not shown). This variability is not surprising, considering introduction of MTS-ES increases negative charge within the cation-selective channel while also introducing steric bulk which may hinder ion flow. Despite this variability, a response to MTS-ES occurred only at positions that were also responsive to MTS-ET. These results, as a whole, support the proposed model of insertion of each D2L2 as a β hairpin.

Single-Channel Measurements. If the proposed model of channel formation is correct, single-channel measurements of MTS-ET-responsive mutants might permit one to resolve individual reactions between MTS-ET and each of the seven single cysteine residues within the heptameric pore. We performed single-channel measurements with two mutants, N306C and H304C. In a typical experiment, trypsin-activated mutant PA was added to a diphytanoylphosphatidylcholine membrane separating identical salt solutions (100 mM KCl) at pH 6.6, and generally a single channel opened within 30 min. The conductance of the N306C and H304C channels was the same as that of wild-type channels (~100 pS at an applied voltage of +50 mV) (*30*). MTS-ET was then added to the trans compartment, the solutions were stirred briefly, and the effect on conductance was observed. With single N306C channels, stepwise jumps to lower conductance states were seen following addition of MTS-ET, consistent with multiple reactions within a multimeric channel (Figure 4A). Furthermore, subsequent addition of DTT reversed the MTS-ET effect: multiple stepwise increases in channel conductance, consistent with DTT-mediated reduction of the mixed disulfide between the cysteines and ethyltrimethylammonium (the product of the MTS-ET reactions), were seen until the original channel conductance was regained (Figure 4B). Similar effects were seen when MTS-ET was added to single channels formed by H304C.

The pattern of conductance inhibition by MTS-ET was similar in all single-channel experiments: a decrease in conductance occurred during or immediately following addition of MTS-ET, and additional jumps to lower conductance states occurred afterward. Up to five transitions

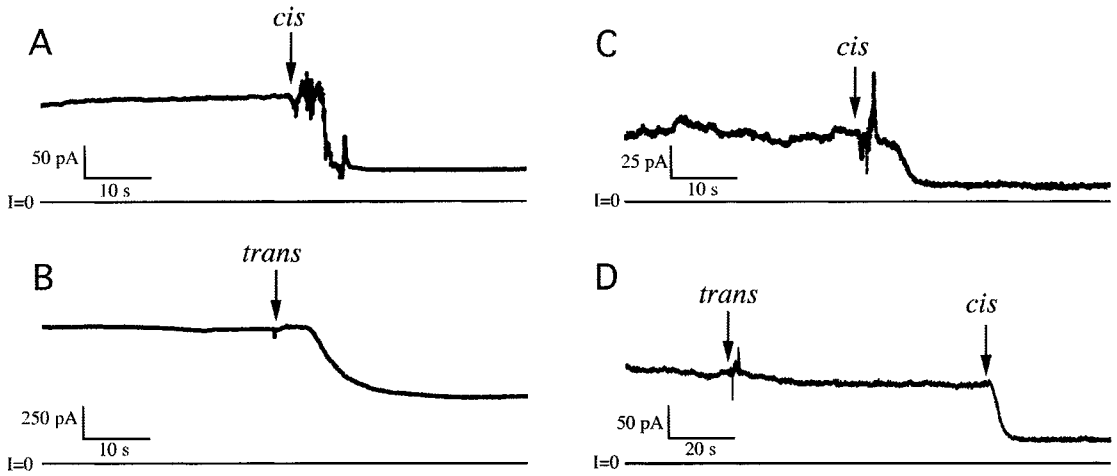

FIGURE 5: MTS-ET restricts the accessibility of trans but not cis Bu_4N^+ to its binding site. Current records (with voltage held at +20 mV) begin 3−5 min after addition of trypsin-nicked PA S325C. The arrows mark addition of Bu_4N^+. (A and B) Addition of Bu_4N^+ to unmodified S325C channels. In (A), the addition of Bu_4N^+ cis to a concentration of 15 μM produced a 3.5-fold fall in conductance; in (B), the addition of Bu_4N^+ trans to a concentration of 500 μM produced a 2-fold fall in conductance. (C and D) Addition of Bu_4N^+ to S325C channels previously modified with MTS-ET. (C) Addition of Bu_4N^+ cis to a concentration of 15 μM produced the same 3.5-fold fall in conductance as in (A), despite the conductance having previously been substantially reduced due to modification of the channels' cysteines with MTS-ET. (D) Addition of 500 μM Bu_4N^+ trans to channels previously reacted with MTS-ET had essentially no effect on conductance; subsequent addition of 15 μM Bu_4N^+ cis produced its usual 3.5-fold fall in conductance. Thus, with the cysteines at positions 325 modified with MTS-ET, Bu_4N^+ added trans is prevented from reaching its binding site, whereas Bu_4N^+ added cis is not. These results argue that the Bu_4N^+ binding site lies cis to position 325.

to lower conductance states were resolved within some single channels. The state of lowest conductance ranged from 28 pS to 12 pS (72−88% reduction), depending upon the experiment, and the magnitudes of individual transitions varied from experiment to experiment. In the putative heptameric channel, 19 spatial combinations would be allowed for derivatization of 1−7 cysteines (*31*). (For instance, the second MTS-ET could modify cysteines at any of three different locations relative to the first—an adjacent residue, or one or two monomers removed.) Each configuration may result in a different reduction of channel conductance through a combination of steric and electrostatic effects.

In the course of performing the experiments described above, the observation was made that reaction with MTS-ET and reversal by DTT could apparently occur from the trans compartment while the channel was temporarily closed. For example, during single-channel experiments with N306C, a channel often transiently closed for a few seconds. In some cases, when the channel closed in the presence of trans MTS-ET, it reopened to a lower conductance state. Similarly, following the addition of DTT, a closed channel sometimes reopened to a higher conductance state (data not shown). Such results imply that D2L2 forms a channel which is gated at a site cis relative to position 306.

MTS-ET Restricts Accessibility to Bu_4N^+ Added trans but Not cis. Symmetric quaternary ammonium ions ranging in size from tetramethyl to tetraheptyl have been shown to block PA_{63} channels in a voltage-dependent manner (*32*). In studies with Bu_4N^+, an approximately 40-fold higher trans concentration at +20 mV was required to yield the same effect as a given cis concentration at that voltage. Macroscopic and single-channel analyses led to a two-barrier single-well energy barrier model for binding of Bu_4N^+ within the PA_{63} channel (*30*, *32*). To test whether one of the residues of D2L2 participates in binding Bu_4N^+, we screened each mutant for the ability to yield a Bu_4N^+ blocking effect. In each mutant, as in wild-type channels, a rapid 2−5-fold reduction of macroscopic current was seen when Bu_4N^+ was added to the cis compartment to a concentration of 15 μM (e.g., Figure 5A). The ability of each mutation to yield a normal Bu_4N^+ blocking effect suggests that the binding site does not involve the D2L2 residues and, therefore, lies elsewhere in the protein.

To investigate if the Bu_4N^+ binding site is located cis with respect to the inserted D2L2, we first reacted channels of S325C, the site proposed to be located furthest cis, with MTS-ET and then determined whether subsequent cis or trans addition of Bu_4N^+ had its usual effect on conductance. We reasoned that electrostatic repulsion from the ethyltrimethylammonium ion bound to reacted cysteines within the channel would inhibit flow of Bu_4N^+ ions past the derivatized region and thereby inhibit its access to its binding site, if the site lay beyond the derivatized region. As seen in Figure 5C, prior reaction with MTS-ET at residue S325C did not prevent subsequent cis 15 μM Bu_4N^+ from producing its usual rapid 3.5-fold fall in conductance, seen in Figure 5A, even though the conductance was already substantially reduced. This by itself strongly suggests that the Bu_4N^+ binding site lies cis relative to D2L2. As further confirmation, prior reaction of S325C with MTS-ET prevented trans 500 μM Bu_4N^+ from producing its usual 2-fold fall in conductance (compare Figure 5D to Figure 5B). One would expect such a result if the Bu_4N^+ binding site lies cis relative to residue 325, as the ethyltrimethylammonium ion bound to reacted cysteines at that site would inhibit trans Bu_4N^+ from reaching its binding site. These results strongly suggest that the Bu_4N^+ binding site is located cis relative to D2L2, presumably within the putative globular cap region of the pore.

DISCUSSION

Although many bacterial toxins act by modifying cytosolic substrates within the mammalian cell, we presently do not

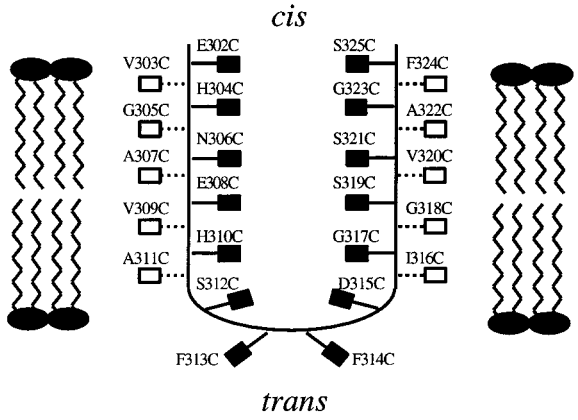

FIGURE 6: Model for the orientation of D2L2 within the membrane. The filled boxes indicate residues that are responsive to MTS-ET, based upon reduction of channel conductance. The open boxes indicate residues that show little or no effect upon MTS-ET addition. The pattern is consistent with each D2L2 contributing two antiparallel β strands to make a 14-stranded β barrel.

understand how the enzymic moiety crosses a membrane for any toxin. In some A−B toxins, such as diphtheria and anthrax toxins, the B moiety inserts into membranes under translocation conditions to form a pore which may serve as a conduit for A-chain translocation. To probe this hypothesis effectively, it is essential to understand the structure of the pore in detail. The recently solved crystal structure of the heptameric PA_{63} prepore of anthrax toxin has provided a detailed structure of an intermediate in pore formation (*6*). In this study, we have tested a model of prepore-to-pore conversion involving formation of a transmembrane 14-stranded β barrel from the D2L2 loop of domain 2. The results presented represent strong evidence in favor of the model.

We used the substituted cysteine accessibility method (*20*) to test whether single cysteines within the D2L2 loop were brought into direct contact with the lumen of the ion-conducting channel upon conversion to the pore. The probe used, MTS-ET, has been shown to be bilayer-impermeant by liposome leakage and excised patch experiments (*33*), and derivatization of cysteines by methanethiosulfonate reagents has been shown to occur 10 orders of magnitude faster when cysteine is in the hydrated thiolate anion form rather than the sulfhydryl form (*34*). Thus, only solvent-accessible cysteines would be expected to react with the reagent. Also, since the diameter of the PA_{63} channel has been estimated at 12 Å in channel blockage experiments (*35*), whereas the diameter of MTS-ET is only 6 Å (*20*), we expected residues lining the channel to be accessible to the reagent. Finally, if a cysteine lining the ion conducting pathway reacted with MTS-ET, the introduction of positive charge would be likely to inhibit ion conductance within the cation-selective PA_{63} channel.

The pattern of inhibition of macroscopic conductance by MTS-ET was strikingly close to that predicted by the model (Figure 6). Alternating residues within each of two stretches (302−311, 316−325) that had been predicted to form the antiparallel strands of the β barrel showed different effects following addition of the reagent. Residues predicted to lie on the polar, luminal face of the barrel showed strong reduction of conductance by MTS-ET, whereas those predicted to lie on the apolar, membrane-contiguous face showed little to no reduction. The lack of effect in the latter case most likely reflects inaccessibility to the reagent. The two regions of alternating accessibility were bridged by a short segment of fully accessible residues (residues 312−315) that encompass the residues which had been predicted to form the β turn of the putative hairpin (Figure 1A). Two aromatic residues in this region, F313 and F314, presumably border the membrane/water interface at the trans face of the bilayer. Aromatic residues have been shown to lie at the lipid/water interface and girdle β barrels formed by porins, as seen in the crystal structure of a porin from *Rhodopseudomonas blastica* (*36*). The β turn region within D2L2 of protective antigen is presumably different than that adopted by the *Staphylococcus aureus* α-hemolysin: in PA_{63}, the *i* and *i*+3 residues of the turn need to lie on the same face of the hairpin, while in the α-hemolysin, *i* and *i*+3 apparently lie on opposite sides of the barrel. Only two minor anomalies in the overall pattern of inhibition were observed: in some experiments, a weak effect of MTS-ET was detected at A307C and I316C. This may reflect greater flexibility of the β structure at these locations.

The absence of an MTS-ET effect at hydrophobic positions in D2L2 does not, of course, prove that these residues face the interior of the bilayer. It is conceivable that one or more of these positions are in contact with the channel, but their reactivity is inhibited by other mechanisms; alternatively, reactions may occur but have no effect on conductance at these positions. It is also possible that these residues form the exterior surface of a channel segment which does not penetrate the membrane. The consistent pattern to the MTS-ET effects, however, makes these possibilities unlikely. Further work is underway employing electron paramagnetic resonance and fluorescence to test our assumption that the apparently nonreactive residues lie within a lipid environment.

Also consistent with the proposed model are the results of single-channel measurements, showing multiple stepwise conductance changes in response to MTS-ET at positions 306 and 304. The stepwise changes were reversible with DTT and were consistent with single reaction events involving individual cysteines in the channel. The data imply that the channel is comprised of an oligomeric structure, correlating with the heptameric, ring-shaped structure of PA_{63} observed by electron microscopy and X-ray crystallography (*6*, *10*). We resolved up to five MTS reactions per channel, but this probably does not reflect the maximum number of protomeric cysteines lining the pore. Because each successive MTS-ET reaction lowers conductance by introducing greater electrostatic repulsion and steric constraints within the channel, derivatization of all cysteines may not have been possible within the time frame of a normal experiment.

The variation in stepwise changes in conductance from experiment to experiment may reflect the large number of possible configurations of reacted cysteines within the channel. Up to 19 configurations of 1−7 reacted cysteines within a heptamer are theoretically possible (*31*), and each configuration may have a unique effect on conductance resulting from steric and electrostatic effects. Multiple MTS reactions within a single channel have also been observed in analysis of the ryanodine receptor channel (*37*), where four discrete subconductance states of 3/4, 1/2, 1/4, and 0-fold of the unreacted channel were seen. In contrast,

single-channel analysis of the effects of MTS reagents on cysteine-substituted channels formed by the diphtheria toxin T domain has revealed only one stepwise change in conductance per channel, consistent with a single MTS reaction within a monomeric channel (*26*).

According to the proposed model for channel formation by PA_{63}, the D2L2 loops move to the base of the heptameric prepore, where they form a membrane-inserted β barrel (*6*). The globular domains of the heptameric ring would then extend the pore above the cis leaflet of the membrane, as seen with the *Staphylococcus aureus* α-hemolysin pore. We have found that the channel blocker Bu_4N^+ is prevented from reaching its binding site when added to the trans (but not the cis) compartment of S325C channels prederivatized with MTS-ET. This implies that the binding site for Bu_4N^+ is located cis relative to the inserted D2L2 loops. The lumen of the prepore is predominantly negatively charged (*6*), and assuming there is little change in that lumen during the prepore-to-pore conversion, it represents a likely locus for binding of the Bu_4N^+ ion. In addition, the ability of trans MTS-ET and DTT to react within the channel in its closed state suggests that the gate lies cis to the membrane-inserted region defined here, and this gate may also reside within the globular cap of the pore.

Within the heptameric prepore, the D2L2 loops are located midway up the globular domains and are flanked by the 2β2 and 2β3 strands of domain 2. For D2L2 to move to the base of the prepore to form the β barrel, it has been proposed that 2β2 and 2β3 tear away from the body of domain 2 under the influence of low pH (*6*). Residues of the 2β2 and 2β3 strands may also contribute to the channel by forming an extension of the β barrel formed by D2L2, and this extension may serve as a link between the membrane-inserted and globular regions. This extension represents an alternative locus for Bu_4N^+ and/or channel gating sites.

Pore-forming bacterial toxins undergo a variety of conformational changes in the transition from a secreted hydrophilic protein to one capable of penetrating a hydrophobic membrane. Such transitions may involve the creation of entirely new surfaces, such as the β barrel for anthrax protective antigen (this work) and for the membrane-associated α-hemolysin (*7*). Another well-documented insertion mechanism involves exposure of a buried amphipathic α-helical hairpin within the native water-soluble protein, as demonstrated for diphtheria toxin (*4*, *38*) and pore-forming colicins (*2*). Dimer dissociation and proteolytic cleavage have been proposed to reveal hydrophobic patches and mediate membrane insertion of the pore-forming toxin aerolysin (*5*). The recently solved crystal structure of a thiol-activated cytolysin, perfringolysin O (PFO), suggests a novel mechanism of insertion in which the binding of PFO to its cholesterol receptor displaces a hydrophobic loop which initiates insertion. Complete penetration of the membrane-inserting domain would then be aided by shielding of a polar face of a β sheet by the cholesterol receptor (*39*).

Of these pore-forming toxins, diphtheria and anthrax protective antigen also translocate an enzymatic moiety into the cytoplasm of mammalian cells. Whether the channel is a route of translocation or a consequence of a translocation-competent state is unknown, but the identification of channel-lining residues in the anthrax protective antigen channel should now facilitate investigation of the role of channel formation in the translocation process.

ACKNOWLEDGMENT

We thank Can Cui for establishing the conditions for expression of PA in *E. coli*, Dr. Jianmin Zhao for construction and purification of the H304C and G305C mutants, and Drs. Carlo Petosa and Robert C. Liddington for discussions and release of PA coordinates prior to publication.

REFERENCES

1. Gill, D. M. (1978) in *Bacterial toxins and cell membranes* (Jeljaszewicz, J., and Wadstrom, T., Eds.) pp 291−322, Academic Press, New York.
2. Parker, M. W., Pattus, F., Tucker, A. D., and Tsernoglou, D. (1989) *Nature 337*, 93−96.
3. Li, J. D., Carroll, J., and Ellar, D. J. (1991) *Nature 353*, 815−821.
4. Choe, S., Bennett, M. J., Fujii, G., Curmi, P. M., Kantardjieff, K. A., Collier, R. J., and Eisenberg, D. (1992) *Nature 357*, 216−222.
5. Parker, M. W., Buckley, J. T., Postma, J. P., Tucker, A. D., Leonard, K., Pattus, F., and Tsernoglou, D. (1994) *Nature 367*, 292−295.
6. Petosa, C., Collier, R. J., Klimpel, K. R., Leppla, S. H., and Liddington, R. C. (1997) *Nature 385*, 833−838.
7. Song, L., Hobaugh, M. R., Shustak, C., Cheley, S., Bayley, H., and Gouaux, J. E. (1996) *Science 274*, 1859−866.
8. Escuyer, V., and Collier, R. J. (1991) *Infect. Immun. 59*, 3381−3386.
9. Klimpel, K. R., Molloy, S. S., Thomas, G., and Leppla, S. H. (1992) *Proc. Natl. Acad. Sci. U.S.A. 89*, 10277−10281.
10. Milne, J. C., Furlong, D., Hanna, P. C., Wall, J. S., and Collier, R. J. (1994) *J. Biol. Chem. 269*, 20607−20612.
11. Leppla, S. H., Friedlander, A. M., and Cora, E. M. (1988) in *Bacterial Protein Toxins* (Ferenbach, Ed.) pp 111−112, Gustav Fisher, Stuttgart.
12. Gordon, V. M., Leppla, S. H., and Hewlett, E. L. (1988) *Infect. Immun. 56*, 1066−1069.
13. Friedlander, A. M. (1986) *J. Biol. Chem. 261*, 7123−7126.
14. Leppla, S. H. (1982) *Proc. Natl. Acad. Sci. U.S.A. 79*, 3162−3166.
15. Hanna, P. C., Acosta, D., and Collier, R. J. (1993) *Proc. Natl. Acad. Sci. U.S.A. 90*, 10198−10201.
16. Blaustein, R. O., Koehler, T. M., Collier, R. J., and Finkelstein, A. (1989) *Proc. Natl. Acad. Sci. U.S.A. 86*, 2209−2213.
17. Koehler, T. M., and Collier, R. J. (1991) *Mol. Microbiol. 5*, 1501−1506.
18. Milne, J. C., and Collier, R. J. (1993) *Mol. Microbiol. 10*, 647−653.
19. Gouaux, J. E., Braha, O., Hobaugh, M. R., Song, L., Cheley, S., Shustak, C., and Bayley, H. (1994) *Proc. Natl. Acad. Sci. U.S.A. 91*, 12828−12831.
20. Akabas, M. H., Stauffer, D. A., Xu, M., and Karlin, A. (1992) *Science 258*, 307−310.
21. Akabas, M. H., Kaufmann, C., Archdeacon, P., and Karlin, A. (1994) *Neuron 13*, 919−927.
22. Xu, M., and Akabas, M. H. (1996) *J. Gen. Physiol. 107*, 195−205.
23. Cheung, M., and Akabas, M. H. (1996) *Biophys. J. 70*, 2688−2695.
24. Pascual, J. M., Shieh, C. C., Kirsch, G. E., and Brown, A. M. (1995) *Neuron 14*, 1055−1063.
25. Wang, K. W., Tai, K. K., and Goldstein, S. A. (1996) *Neuron 16*, 571−577.
26. Huynh, P. D., Cui, C., Zhan, H., Oh, K. J., Collier, R. J., and Finkelstein, A. (1997) *J. Gen. Physiol. 110*, 229−242.
27. Montal, M. (1974) *Methods Enzymol. 32*, 545−554.

28. Wonderlin, W. F., Finkel, A., and French, R. J. (1990) *Biophys. J. 58*, 289−297.
29. Silverman, J. A., Mindell, J. A., Zhan, H., Finkelstein, A., and Collier, R. J. (1994) *J. Membr. Biol. 137*, 17−28.
30. Blaustein, R. O., Lea, E. J., and Finkelstein, A. (1990) *J. Gen. Physiol. 96*, 921−942.
31. Braha, O., Walker, B., Cheley, S., Kasianowicz, J. J., Song, L., Gouaux, J. E., and Bayley, H. (1997) *Chem. Biol. 4*, 497−505.
32. Blaustein, R. O., and Finkelstein, A. (1990) *J. Gen. Physiol. 96*, 905−919.
33. Holmgren, M., Liu, Y., Xu, Y., and Yellen, G. (1996) *Neuropharmacology 35*, 797−804.
34. Roberts, D. D., Lewis, S. D., Ballou, D. P., Olson, S. T., and Shafer, J. A. (1986) *Biochemistry 25*, 5595−5601.
35. Finkelstein, A. (1994) *Toxicology 87*, 29−41.
36. Kreusch, A., Neubuser, A., Schiltz, E., Weckesser, J., and Schulz, G. E. (1994) *Protein Sci. 3*, 58−63.
37. Quinn, K. E., and Ehrlich, B. E. (1997) *J. Gen. Physiol. 109*, 255−264.
38. Oh, K. J., Zhan, H., Cui, C., Hideg, K., Collier, R. J., and Hubbell, W. J. (1996) *Science 273*, 810−812.
39. Rossjohn, J., Feil, S. C., McKinstry, W. J., Tweten, R. K., and Parker, M. W. (1997) *Cell 89*, 685−692.

BI972657B